



LAWRENCE  
LIVERMORE  
NATIONAL  
LABORATORY

# Frequency distribution, isotopic composition and physical characterization of plutonium-bearing particles from the Fig-Quince zone on Runit Island, Enewetak Atoll

T.F. Hamilton, J. Jernstroem, R. E. Martinelli, S.R. Kehl, M. Eriksson, R. W. Williams, M. Bielewski, A. Rivers, T.A. Brown, S.J. Tumey, M. Betti

April 15, 2009

Journal of Radioanalytical and Nuclear Chemistry

## **Disclaimer**

---

This document was prepared as an account of work sponsored by an agency of the United States government. Neither the United States government nor Lawrence Livermore National Security, LLC, nor any of their employees makes any warranty, expressed or implied, or assumes any legal liability or responsibility for the accuracy, completeness, or usefulness of any information, apparatus, product, or process disclosed, or represents that its use would not infringe privately owned rights. Reference herein to any specific commercial product, process, or service by trade name, trademark, manufacturer, or otherwise does not necessarily constitute or imply its endorsement, recommendation, or favoring by the United States government or Lawrence Livermore National Security, LLC. The views and opinions of authors expressed herein do not necessarily state or reflect those of the United States government or Lawrence Livermore National Security, LLC, and shall not be used for advertising or product endorsement purposes.

## LOG # 263

### **Frequency distribution, isotopic composition and physical characterization of plutonium-bearing particles from the Fig-Quince zone on Runit Island, Enewetak Atoll**

T.F. Hamilton<sup>1,\*</sup>

<sup>1</sup>Center for Accelerator Mass Spectrometry, Lawrence Livermore National Laboratory,  
P.O. Box 808, Livermore, CA 94550-0808, USA

[hamilton18@llnl.gov](mailto:hamilton18@llnl.gov)

J. Jernstroem

[jusj@risoe.dtu.dk](mailto:jusj@risoe.dtu.dk)

R. Martinelli

[martinelli2@llnl.gov](mailto:martinelli2@llnl.gov)

S.R. Kehl

[kehl1@llnl.gov](mailto:kehl1@llnl.gov)

M. Eriksson

[M.Eriksson@iaea.org](mailto:M.Eriksson@iaea.org)

R. Williams

[williams141@llnl.gov](mailto:williams141@llnl.gov)

M. Bielewski

[Marek.BIELEWSKI@ec.europa.eu](mailto:Marek.BIELEWSKI@ec.europa.eu)

A. Rivers

[arielrivers@yahoo.com](mailto:arielrivers@yahoo.com)

T. Brown

[tabrown@llnl.gov](mailto:tabrown@llnl.gov)

S. Tumey

[tumey2@llnl.gov](mailto:tumey2@llnl.gov)

M. Betti

[m.betti@iaea.org](mailto:m.betti@iaea.org)

---

\*Corresponding author, email: [hamilton18@llnl.gov](mailto:hamilton18@llnl.gov), telephone +1 925 422 6621;  
facsimile +1 925 423 6785

**Frequency distribution, isotopic composition and physical characterization of plutonium-bearing particles from the Fig-Quince zone on Runit Island, Enewetak Atoll**

TERRY HAMILTON<sup>1,\*</sup>, JUSSI JERNSTROEM<sup>2</sup>, ROGER MARTINELLI<sup>1</sup>, STEVEN KEHL<sup>1</sup>,  
MATS ERIKSSON<sup>3</sup>, ROSS WILLIAMS<sup>5</sup>, MAREK BIELEWSKI<sup>4</sup>, ARIEL RIVERS<sup>1</sup>, TOM  
BROWN<sup>1</sup>, SCOTT TUMEY<sup>1</sup>, MARIA BETTI<sup>3</sup>

<sup>1,\*</sup>Center for Accelerator Mass Spectrometry, Lawrence Livermore National Laboratory, P.O. Box 808, Livermore, CA 94550-0808, USA

<sup>2</sup>Radiation Research Division, Risø National Laboratory for Sustainable Energy, Technical University of Denmark (DTU), Building 204, P.O. Box 49, DK-4000 Roskilde, Denmark

<sup>3</sup>IAEA Marine Environment Laboratory (IAEA-MEL), International Atomic Energy Agency, 4 Quai Antoine 1er, BP 800, MC 08012, Monaco Cedex, Principality of Monaco

<sup>4</sup>Institute for Transuranium Elements, EC DG JRC, P.O. Box 2340, 76125 Karlsruhe, Germany

<sup>5</sup>Chemical Sciences Division, Lawrence Livermore National Laboratory, P.O. Box 808, Livermore, CA 94550-0808, USA

**Abstract**

Runit Island on Enewetak Atoll was very heavily impacted by the U.S. nuclear testing campaign in the northern Marshall Islands (1946-58). The primary source of contamination on Runit Island was the 1958 Quince *safety test* where a large quantity of device plutonium (Pu) was scattered over the area near the GZ. A second low-yield device was detonated on the same site 10 days later, further disturbing the soil and leaving behind a very heterogeneous pattern of contamination including milligram-size particles of plutonium. A limited cleanup of the Fig-Quince zone was carried out in 1979. During this period, the effectiveness of the cleanup operations was primarily evaluated on the basis of bulk soil concentration data with little consideration given to the heterogeneity and long-term material-, biological-, and environmental-specific impacts of residual high activity (hot) particle contamination. The aim of the present study was twofold; (i) to characterize the levels and distribution of residual contamination in the

Fig-Quince zone, and (ii) to develop pertinent data on the frequency distribution, elemental and isotopic composition, and physico-chemical properties of hot particles isolated from surface soils from Fig-Quince with a view towards providing recommendations on the future management and possible cleanup of the site. Today, Runit Island remains under an administrative quarantine.

**Key words:** radioactive particles,  $^{238}\text{Pu}$ ,  $^{239}\text{Pu}$ ,  $^{240}\text{Pu}$ ,  $^{241}\text{Pu}$ ,  $^{242}\text{Pu}$ ,  $^{244}\text{Pu}$ ,  $^{241}\text{Am}$ , Runit Island, Enewetak Atoll, Marshall Islands, gamma-spectrometry, SR- $\mu$ -XRF, SEM-EDX, SIMS, MCICP-MS, AMS, soil particle size fractionation.

## INTRODUCTION

During the period between 1948 and 1958, the U.S. detonated 42 atmospheric nuclear weapons tests in the near-surface environment of Enewetak Atoll in the northern Marshall Islands.<sup>1</sup> The test program produced close-in fallout deposition that contaminated islands and the local atoll lagoon environment with a range of fission and activation products, and unfissioned nuclear fuel.<sup>2,3</sup> Runit Island experienced eight ground surface tests, eight barge tests conducted from anchor points in the nearby lagoon and on the ocean reef, and one targeted airdrop.<sup>4</sup> However, the most significant contaminating event on Runit was the 1958 Quince test which dispersed device plutonium without reaching criticality in what was commonly described as a *safety test*. According to various historical reports, contaminated soil from the Quince event was supposedly dumped into the lagoon or bulldozed towards the shoreline, and covered with uncontaminated soil in preparations for the Fig test.<sup>4</sup> The Fig event produced little or no fission yield but contributed to the heterogeneous nature of radioactive contamination in the Fig-Quince zone. The discovery of discrete pieces of plutonium-contaminated beryllium as well as milligram-size and larger radioactive fragments prompted a cleanup of the site during 1979. Approximately 266 GBq of TRU activity ( $^{238+239+240}\text{Pu}$  and  $^{241}\text{Am}$  = TRU) contained in 8,200 m<sup>3</sup> of soil was recovered from the Fig-Quince zone in 1979 and entombed inside Cactus Crater on

the north end of the island. The existence of a Low-Level Radioactive Waste Repository (known as *Runit Dome*) on Runit Island is a lingering concern for the local leadership and the people of Enewetak Atoll. There is no established program for monitoring of leakage from Runit Dome but the risk posed by redistribution of the entire inventory of the waste pile into the lagoon is relatively low when compared to the existing levels of contamination in the marine environment.<sup>2,5</sup> Moreover, the likelihood of such a catastrophic release occurring is very low<sup>5</sup>. Today, there is a more immediate concern from residual fallout contamination in the terrestrial environment and the associated risk from inhalation and/or dermal exposure to contaminated soil particles. Levels of TRU contamination ( $\text{TRU} = {}^{238,239,240}\text{Pu} + {}^{241}\text{Am}$ ) on central Runit within the Fig-Quince zone are higher than at any other location in the Marshall Islands. Also, we have recently learnt that some local workers have been digging in the soil on central Runit in an effort to recovery copper wiring for its scrap metal resale value. The known heterogeneity and existence of plutonium-bearing particles on Runit Island only tends to exasperate the problem because the availability of particulate forms of plutonium (as well as for other actinide elements) to undergo further interactions in the environment will be strongly influenced by the physical nature, composition and transport behavior of the host particles as well as the physico-chemical properties of the particle associated radionuclides. The dose commitment following an intake of a radioactive particle will also depend on the *in vitro* dissolution kinetic of particles, and the behavior of the different forms of radionuclides in the body.<sup>6,7</sup>

In general, radioactive particles are now understood to be much more prevalent in the environment than previously postulated, and present new challenges in the fields of radioecology, risk assessments and environmental cleanup.<sup>8,9,10</sup> A number of refined analytical techniques are available to study the size, elemental and isotopic composition, surface

morphology, and physico-chemical properties of high activity particles.<sup>8-23</sup> For example, the elemental distribution within single grains can be determined using  $\mu$ -beam X-ray emission techniques such as SEM-EDX, SR- $\mu$ -XRF, PIXE, and  $\mu$ -XRF, and the 3-D distribution of particles may be determined using confocal  $\mu$ -XRF and  $\mu$ -tomography. In addition, speciation and determination of oxidation states of U and Pu is made possible by using of SR- $\mu$ -XANES and SR- $\mu$ -XRD. The application of these techniques together with the use of more conventional methods such low-energy gamma-spectrometry and mass-spectrometry (e.g., SIMS, MCICP-MS, AMS) has been invaluable in helping improve our understanding of the physical nature and composition of high-activity particles in the environment.<sup>8,9,10,14,18,19,20,21,24,25</sup> This paper provides an overview of the application of these techniques in relation to the radiological situation at Runit Island with emphasis on the initial investigation designed to assess the levels, distribution and particle size fractionation of plutonium in soils from the Fig-Quince zone. The long-term strategic goal of these studies is to develop source-specific data and information which might prove helpful in making more informed decisions about the long-term management and possible future cleanup of the site.

## **EXPERIMENTAL**

### **Sample collection and handling**

The geographical location of the Fig-Quince zone (approximately 3 hectares in area) on central Runit was identified using map references from historical reports.<sup>4</sup> The site was initially surveyed on a 20 m grid pattern using a Model 935 Surveillance and Measurement System (SAM) *in-situ* gamma spectrometer (from Berkeley Nucleonics, Inc.) equipped with a NaI detector. Surface soils were collected from each of the grid point locations. Separate soil profiles (at 0-5 cm, 5-10 cm, 10-15 cm, and 15-25 cm) were collected for hot particle studies from five

sites identified as containing elevated levels of  $^{241}\text{Am}$  contamination from the *in-situ* gamma survey. Additional *hot particle* spot samples were collected by narrowly defining the location of a particle by slowly moving the face of the detector across the surface of the soil, and then removing the particle with small quantities of soil until the remaining activity dropped. All soil samples were packaged in the field and stored frozen for shipment to the Lawrence Livermore National Laboratory (LLNL).

#### Hot-particle distribution and isotopic analysis

At LLNL, the soil samples were initially oven dried at 60 °C to constant weight, and then processed according to the following protocol. Grid samples were pulverized by ball-milling to produce a finely divided powder. The powder was then placed in a 200 mL standard tuna can counting geometry, and analyzed for gamma emitting radionuclides ( $^{60}\text{Co}$ ,  $^{137}\text{Cs}$ , and  $^{241}\text{Am}$ ) using conventional high-resolution gamma-spectrometry.

Depth profile samples were partitioned into 50 g sub-aliquots (normally 70–90 individual samples each) and the material placed in plastic sample jars. Each sample jar was then screened for the presence of  $^{241}\text{Am}$  using a portable gamma spectrometry (SAM) unit as described above with added shielding for the detector. Those samples showing higher-than-average count rates were successively split to obtain individual high-activity particles contained in 50 to 250 mg of soil. The  $^{241}\text{Am}$  content of the each high activity particle sample was determined by high-resolution gamma-spectrometry, and the material reserved for non-destructive analysis.

The remaining material from the high-activity particle isolation procedure was recombined, placed in a metal can, and carefully homogenized on a roller. This material was then used for dry sieve analysis. The automated sieve apparatus consisted of a Analysette 3 PRO (FRITSCH) shaker fitted with stacked stainless steel sieves (200 mm diameter) containing 20



$\mu\text{m}$ , 44  $\mu\text{m}$ , 125  $\mu\text{m}$ , 500  $\mu\text{m}$ , 1.2 mm and 4.8 mm mesh widths. The dry sieve analysis was performed in triplicate using between 250 and 300 g of soil. The fractioned soil from each mesh size was weighed separately and the % soil within each mesh size reported as the arithmetic mean and standard deviation. The fractions from each mesh size for each sample were then recombined and homogenized by rolling or pulverized by ball milling. Each size fraction was then analyzed for plutonium isotopes ( $^{239}\text{Pu}$ ,  $^{240}\text{Pu}$ ,  $^{241}\text{Pu}$ ) using MCICP-MS. Grid samples were also prepared and analyzed for plutonium isotopes. Details concerning the MCICP-MS analysis of soils at LLNL under the Marshall Islands Program are given elsewhere.<sup>26</sup> A more detailed analysis of uranium ( $^{234}\text{U}$ ,  $^{235}\text{U}$ ,  $^{236}\text{U}$ ,  $^{238}\text{U}$ ) and plutonium isotopes ( $^{238}\text{Pu}$ ,  $^{239}\text{Pu}$ ,  $^{240}\text{Pu}$ ,  $^{241}\text{Pu}$ ,  $^{242}\text{Pu}$ ,  $^{244}\text{Pu}$ ) on a composite soil sample from Fig-Quince was performed using a combination of alpha-spectrometry, MCICP-MS and AMS.

*Non-destructive analysis of high-activity particles (at collaborating institutions)*

The high-activity particle samples obtained from LLNL were further segregated ( $\sim\mu\text{g}$ ) at the Institute for Transuranium Elements (ITU) using a sample splitting technique, placed on adhesive carbon tape, and the exact location of individual high-activity grains revealed with a beta camera.<sup>27</sup> Surface morphology and elemental composition of the individual grains were studied by analyzing the X-ray fluorescence signal from an SEM equipped with an energy dispersive X-ray (EDX) spectrometer (PERSONAL SEM®, RJ Lee Group, Inc., USA). The SEM-EDX was operated in the backscatter mode with an applied voltage of 20 kV at a filament-to-sample distance between 16 and 18 mm.<sup>24</sup> 3-D maps of the elemental composition (at 10-50  $\mu\text{m}$  resolution) of the high-activity grains were obtained by SR- $\mu$ -XRF using the ANKA FLUO beam line at the Synchrotron Radiation Facility situated in Karlsruhe, Germany.<sup>28</sup> The intensity maps correspond to Pu-L $\alpha$  X-ray lines. A compound refractive lens (CRL) was used to focus the

exciting beam and the polycapillary half lens to collimate the detector. SIMS studies were conducted with a double-focusing CAMECA IMS 6f (Courbevoie, France) spectrometer. This instrument uses fast switching between masses, and two microfocus ion sources which can be used in either a microscope or microprobe mode.<sup>24,29</sup> SIMS techniques were found to be well suited to studying the depth distribution of radionuclides in isolated single grain particles without the need for radiochemical separation.

## RESULTS AND DISCUSSION

The mean residual activity concentration of  $^{137}\text{Cs}$ ,  $^{241}\text{Am}$  and  $^{239+240}\text{Pu}$  in surface soils from the grid point locations on Fig-Quince averaged  $30 \pm 28 \text{ Bq kg}^{-1}$ ,  $268 \pm 119 \text{ Bq kg}^{-1}$ , and  $1443 \pm 587 \text{ Bq kg}^{-1}$  (dry soil), respectively (Table 1). Duplicate measurements of  $^{239+240}\text{Pu}$  in soil show that the analyses of plutonium by MCICP-MS were surprisingly reproducible given the known heterogeneity of the soil and the small size aliquots (1 g) used in the analysis. The average coefficient of variance for 10 replicate measurements was 4.2% with one outlier at 88% (T. Hamilton, unpublished data). The  $^{240}\text{Pu}/^{239}\text{Pu}$  atom ratio in surface soil from Fig-Quince averaged  $0.062 \pm 0.008$  and is representative of weapons grade or low-yield device plutonium.<sup>4</sup> No clear trends were observed in the activity concentration of  $^{239+240}\text{Pu}$  with increasing depth but significant levels of plutonium contamination extended down to 25 cm in 4 of the 5 soil profiles (Table 2). It is also our understanding that during the final stages of the 1979 cleanup of Runit Island, the Fig-Quince zone was graded over to remove hummocks and covered with a layer of “relatively low TRU activity” soil removed from an area just south of the GZ near the 1310 bunker. Such actions would have contributed to heterogeneous nature of contamination on Fig-Quince and suggests that higher levels of contamination may be found in deeper segments of the soil.

The results of a full isotope analysis of a composite soil sample from Fig-Quince are shown in Table 3. The % abundance of  $^{238}\text{Pu}$ ,  $^{239}\text{Pu}$ ,  $^{240}\text{Pu}$ ,  $^{241}\text{Pu}$  and  $^{242}\text{Pu}$  are almost identical to that reported by the US DOE for *assumed* weapons grade plutonium after applying the necessary decay corrections for shorter lived isotopes.<sup>4</sup> With the exception of finding detectable levels of uranium-236 ( $^{236}\text{U}$ ), the total uranium content and isotopic composition of this composite soil are more consistent with natural background levels in coral atoll soils.<sup>32</sup> The natural abundance of  $^{236}\text{U}$  in the environment is very low with current estimates around  $1\text{-}1000 \times 10^{-14}$  atoms %. The origin of  $^{236}\text{U}$  in soils from Fig-Quince is not clear but presumably was either in the original device material (potentially as a contaminant) or formed *in-situ* as a result of neutron capture reactions on  $^{235}\text{U}$ .

The identification of a high-activity particle or particles in a soil sample was operational defined as containing a significantly elevated  $^{241}\text{Am}$  count rate above the normal sample background. Using this definition, the limit of detection for high-activity particles in a 50 g sample ranged from about 5 to 20 Bq of  $^{241}\text{Am}$ . The frequency distribution of high activity particles was estimated by examining plots of the  $^{241}\text{Am}$  counts, identifying which 50 g sub-aliquots contained high-activity particles (higher number of counts relative to the background), and then identifying how many high activity particles were present by repeatedly splitting the sample into small and smaller size sub-aliquots. An example plot of  $^{241}\text{Am}$  counts on 50 g sub-aliquots of soil is shown in Fig. 1. We determined that this soil profile contained three high-activity particles, all three particles were located in the top 0–5 cm of the soil column in separate 50 g sub-aliquots. The total volume equivalent of soil analyzed was approximately  $0.67 \text{ dm}^3$ , providing around 344 particles per  $\text{m}^3$  of soil. The majority of high-activity particles recovered from Fig-Quince soil contained between 150 and 350 Bq of  $^{239+240}\text{Pu}$  with an average value

around 200 Bq (range 100–800 Bq). This implies that high-activity particles (operationally defined as above) make up a relatively minor fraction (about 8%) of the total plutonium soil inventory in this sample. Some soils samples were much more heterogeneous and contained up to 1000 particles per m<sup>3</sup>. However, the activity of these particles tended to be smaller so the proportion of plutonium carried in high activity particles remained much the same (conservatively estimated to be in the range of 5 to 15%). This contrasts with work from other sites where most of the activity is carried by relatively few larger-sized particles based on the radioactive particles being log-normally distributed.<sup>32,33</sup> One possible explanation for this difference is that Fig-Quince has already undergone a significant cleanup where highly contaminated soil containing hot particles and larger size fragments were selectively removed.

In general, the findings from this study have important implications for the future cleanup of the site. Given the relatively small size (app. 200 Bq) and low frequency distribution of high-activity particles (5-15%), it may be difficult to utilize RAD detection technologies to separate the soil into high and low activity spoil piles similar to what was done as a waste volume reduction measure for the cleanup program on Johnson Atoll and elsewhere. Moreover, if the bulk of the plutonium is contained in more finely divided particles then any disturbance of the soil to selectively remove high-activity particles will not only have a limited effect on reducing the total plutonium inventory but will most likely increase the dispersion of the radioactive particles and increase the associated risk from inhalation exposure for cleanup workers and local residents.

A similar conclusion is reached by examining the results of the sieve analysis (Table 4). The activity concentration of <sup>239+240</sup>Pu in the <20 µm sieve size fraction for 5 soil samples examined ranged from 2290 Bq kg<sup>-1</sup> to over 15,000 Bq kg<sup>-1</sup>. The soil enhancement factor in the

specific activity of  $^{239+240}\text{Pu}$  in the fine material versus the mean value in surface soils ranged from 2 to 6. Again, any disturbance of the soil through additional cleanup activities or agricultural practices may lead to more widespread dispersion of contaminated soil and increase the potential risk from inhalation exposure. Similarly, physical movement of the soil will tend to increase the friability of the plutonium-bearing particles, and accelerate the rate of weathering and solubility of particle bound radionuclides.

The results of non-destructive analyses based  $\mu$ -beam X-ray emission techniques such as SEM-EDX and  $\mu$ -XRF as well as confocal SR- $\mu$ -XRF and  $\mu$ -XANES indicate that there are two primary types of high activity particles in soils from Fig-Quince.<sup>25,35,36</sup> Type 1 particles contain a compact Pu-rich matrix (and surface) with some heterogeneity and tend to be poorly coated with Ca, O, and Mg (Fig 2). Type 2 particles are more heterogeneous in nature and contain a Si,O-rich matrix (and surface coating) with minor contributions from Al, Ca, Na, and Mg. The plutonium contained in Type 2 particles exists as a particle-like structure or is distributed in the Si,O-rich matrix. The origin of Si based material in a coral soil matrix is uncertain. Type 2 particles also appear to contain trace amounts of  $^{137}\text{Cs}$  suggesting that these particles formed during a fission (low-yield) event, most probably from the Fig test. The coating of particles may help reduce natural weathering rates, and potentially help block the release of particle bound radionuclides into the environment. Such processes are yet to be fully understood but may be of interest in remediation of radioactively contaminated sites. Also,  $\mu$ -XANES analyses based on synchrotron excitation provide confirmatory evidence that the Pu-rich particles contain plutonium in the less soluble 4+ oxidation state.<sup>26</sup>

## CONCLUSION

The Fig-Quince zone on Runit Island is heterogeneously contaminated with device plutonium from nuclear weapons testing. The mean activity concentration of  $^{239+240}\text{Pu}$  in surface soil in the Fig-Quince zone is around  $1.44 \text{ kBq kg}^{-1}$  with a range between 500 and  $3000 \text{ kBq kg}^{-1}$ . Non-destructive analytical techniques based on SEM-EDX and  $\mu$ -XRF clearly show that the soils within Fig-Quince contain discrete plutonium-bearing particles, and that these particles were potentially derived from two different source terms. We suggest that the relatively small size (mean value  $\approx 200 \text{ Bq}$ ) and low frequency distribution (estimated 5-15%) of high activity particles in soils from Fig-Quince will potentially limit the availability of options for future cleanup of the site based on the selective removal of radioactive particles. Moreover, the partitioning of plutonium in the finer mesh size soil provides added concern that any disturbance of the aged soil will tend to re-suspend plutonium-bearing particles and increase the risk from inhalation exposure. Friability of the aged particle matrix may also be a long-term concern, and enhance the mobility and solubility of particulate bound plutonium. The observation that some high activity soil particles contain a surface coating is of special interest because these coatings may limit the effects of weathering on the particles, and reduce the ability for particle bound radionuclides to interact with the environment.

## ACKNOWLEDGEMENTS

The Lawrence Livermore National Laboratory is operated by Lawrence Livermore National Security, LLC, for the U.S. Department of Energy, National Nuclear Security Administration under Contract DE-AC52-07NA27344.

## REFERENCES

1. UNSCEAR (2000). Sources and Effects of Ionizing Radiation, United States Scientific Committee on the Effects of Atomic Radiation, UNSCEAR 2000 Report to the General Assembly, with Scientific Annexes, Volume 1: Sources, United Nations, New York, 2000, 654 pp.
2. V.E. Noshkin, W.L. Robison, *Health Phys.*, 73 (2007) 234.
3. Hamilton T.F. (2004). Linking legacies of the cold war to arrival of anthropogenic radionuclides in the oceans through the 20th century, In: *Marine Radioactivity*, H.D. Livingston (Editor), Vol. 6, Elsevier Science, Amsterdam, pp 30–87.
4. U.S. DEPARTMENT OF ENERGY, Enewetak Radiological Support Project, Final Report, B. Freisen (Editor), U.S. DOE, Nevada Operations Office, NVO-213, Las Vegas, Nevada, pp 336–369.
5. M.L. DAVISSON, T.F. HAMILTON, Report LLNL-TR-403015, Lawrence Livermore National Laboratory, 2008, 50 pp.
6. J.W. STATCHER, E. ANSOBORILO, A.W. PHIPPS, *Radiat. Prot. Dosim.*, 92 (2000) 201.
7. E. ANSOBORILO, J. STATCHER, *Radiat. Prot. Dosim.*, 92 (2000) 139.
8. B. SALBU, *Radiat. Prot. Dosim.*, 92 (2000) 49.
9. B. SALBU, Actinides in the Environment, In: *Plutonium in the Environment*, A. Kudo (Editor), Vol. 1, Elsevier, 2008, pp 121–138.
10. M. BETTI, M. ERIKSSON, J. JERNSTRÖM, G. TAMBORINI, Analysis of Environmental Radioactivity, In: *Radioactivity in the Environment*, P.P. Povenic (Editor), Vol. 11, Elsevier, 2008, pp 355–370.
11. I.G. MADJOUKOV, K. BURNS, B. MADJOUKOVA, E.I. VAPIREV, T. TSACHEVA, *Radiat. Prot. Dosim.*, 40 (1992) 235.
12. F.J. SADALLS, M.G. SEGAL, N. VICTORVA, *J. Environ. Radioact.*, 18 (1993) 5.
13. M.D. DORRIAN, *Radiat. Prot. Dosim.*, 69 (1997) 117.
14. B. SALBU, T. KREKLING, D. OUGHTON, *Analyst*, 123 (1998) 843.
15. B. SALBU, K. JANSSENS, T. KREKLIN, D. OUGHTON, Micro-X-Ray Absorption Tomography and Micro-XANES for Characterization of Fuel Particles, <http://www.esrf.fr/info/science/highlights/1999/chemistry/xanes.html>.
16. R.G. CUDDIHY, G.L. FINCH, G.J. NEWTON, F.F. HAHN, J.A. MEWHINNEY, S.J. ROTENBERG, D.A. POWERS, *Environ. Sci. Technol.*, 23 (1989) 89.
17. J. VAN DER VEEN, A. VAN DER WIJK, W.G. MOOK, *Nature*, 323 (1996), 399
18. B. SALBU, T. KREKLING, O.C. LIND, D.H. OUGHTON, M. DRAKOPOULOS, A. SIMIONOVICI, I. SNIGIREV, A. SNIGIREV, T. WEITKAMP, F. ADAMS, K. JANSSENS, V.A. KASHPAROV, *Nucl. Instrum. Methods Phys. Res., Sect. A*, 467-468 (2001) 1249.

19. B. SALBU, K. JANSSENS, O.C. LIND, K. PROOST, P.R. DANESI, J. Environ. Radioact., 64 (2003) 167.
20. B. SALBU, O.C. LIND, L. SKIPPERUD, J. Environ. Radioact., 74 (2004) 233.
21. J. JERNSTRÖM, M. ERIKSSON, J. OSÁN, G. TAMBORINI, Sz TÖRÖK, R. SIMON, G. FALKENBERG, A. ALSECZ, M. BETTI, J. Anal. At. Spectrom., 19 (2004) 1428.
22. M. ERIKSSON, J. OSÁN, J. JERNSTRÖM, D. WEGRZYNEK, R. SIMON, E. CHINEACANO, A. MARKOWICZ, S. BAMFORD, G. TAMBORINI, Sz TÖRÖK, G.G. FALKENBERG, A. ALSECZ, H. DAHGAARD, P. WOBRAUSCHEK, C. STRELI, N. ZEOGER, M. BETTI, Spectrochim. Acta, Part B, 60 (2005) 455.
23. R. PÖLLANEN, M.E. KETTERER, S. LEHTO, M. HOKKANEN, T.K. IKAHEIMONEN, T. SIISKONEN, M. MORING, M.P. RUBIO MONTERO, A. MARTIN SANCHEZ, J. Environ. Radioact., 90 (2006) 15.
24. J. JERNSTRÖM, M. ERIKSSON, R. SIMON, G. TAMBORINI, O. BILDSTEIN, R. CARLOS MARQUEZ, S.R. KEHL, T.F. HAMILTON, Y. RANEBO, M. BETTI, Spectrochim. Acta, Part B, 61 (2006) 971.
25. M. BIELEWSKI, M. ERIKSSON, J. HIMBERT, M. BETTI, I.G. FALKENBERG, T.F. HAMILTON, J. Radioanal. Nucl. Chem., (this issue).
26. R.E. MARTINELLI, T.F. HAMILTON, R.W. WILLIAMS, S.R. KEHL, J. Radioanal. Nucl. Chem. (this issue).
27. M. ERIKSSON, L. LJUNGGREN, C. HINDORF, Nucl. Instrum. Method Phys. Res., Sect. A, 488 (2002) 375.
28. R. SIMON, G. BUTH, M. HAGELSTEIN, Nucl. Instrum. Methods Phys. Res., Sect. B, 199 (2003) 554.
29. G. TAMBORINI, M. BETTI, V. FORCINA, T. HIERNAUT, B. GIOVANNONE, L. KOCH, Spectrochim. Acta, Part B, 53 (1998) 1289.
30. Defense Nuclear Agency, The Radiological Cleanup of Enewetak Atoll, Washington DC, 1981, 700 pp.
31. W.L. ROBISON, V.E. NOSHKIN, T.F. HAMILTON, C.L. CONRADO, K.T. BOGEN, Report UCRL-LR-143980, Lawrence Livermore National Laboratory, 2001, 21 pp.
32. M. ERIKSSON, On weapons plutonium in the arctic environment (Thule, Greenland). Ph.D. Thesis, Risø-R-1321, Risø National Laboratory, Roskilde, Denmark, 2002, 146 pp.
33. S.V. SHEVCHENKO, Appl. Radiat. Isot., 61 (2004) 1303.
34. M. BIELEWSKI, M. ERIKSSON, J. HIMBERT, R. SIMON, M. BETTI, T.F. HAMILTON, Annual Report of the Synchrotron Facility ANKA at the Forschungszentrum Karlsruhe, Germany, 2 pp.





## LIST OF FIGURES AND TABLES

Fig 1.  $^{241}\text{Am}$  counts in 50 g sub-aliquots of a soil (0-5 cm, 5-10 cm, 10-15 cm, and 15-25 cm) collected from Site 2 on Fig-Quince.

Fig 2a. SEM image of a Type 1 particle with the corresponding EDX spectra. The small black spot on the particle images (right side image) denotes the position where the EDX spectrum was measured.

Fig 2b.  $\mu$ -XRF Pu intensity map of the Pu-L $\alpha$  X-ray lines for the same particle.

Table 1.  $^{137}\text{Cs}$ ,  $^{241}\text{Am}$ ,  $^{239}\text{Pu}$  and  $^{239+240}\text{Pu}$  activity concentrations, and  $^{240}\text{Pu}/^{239}\text{Pu}$  atom ratios in surface soil samples from grid sites collected from the Fig-Quince zone on Runit Island.

Table 2.  $^{239+240}\text{Pu}$  activity concentrations and  $^{240}\text{Pu}/^{239}\text{Pu}$  atom ratios in soil profiles (0-5 cm, 5-10 cm, 10-15 cm, 15-25 cm) from Fig-Quince on Runit Island.

Table 3. Pu and U isotopic abundance in a composite soil collected from Fig-Quince on Runit Island.

Table 4.  $^{239}\text{Pu}$  and  $^{239+240}\text{Pu}$  activity concentrations,  $^{240}\text{Pu}/^{239}\text{Pu}$  atom ratios and %  $^{239+240}\text{Pu}$  in size fractionated soils from Fig-Quince on Runit Island.

Figure 1

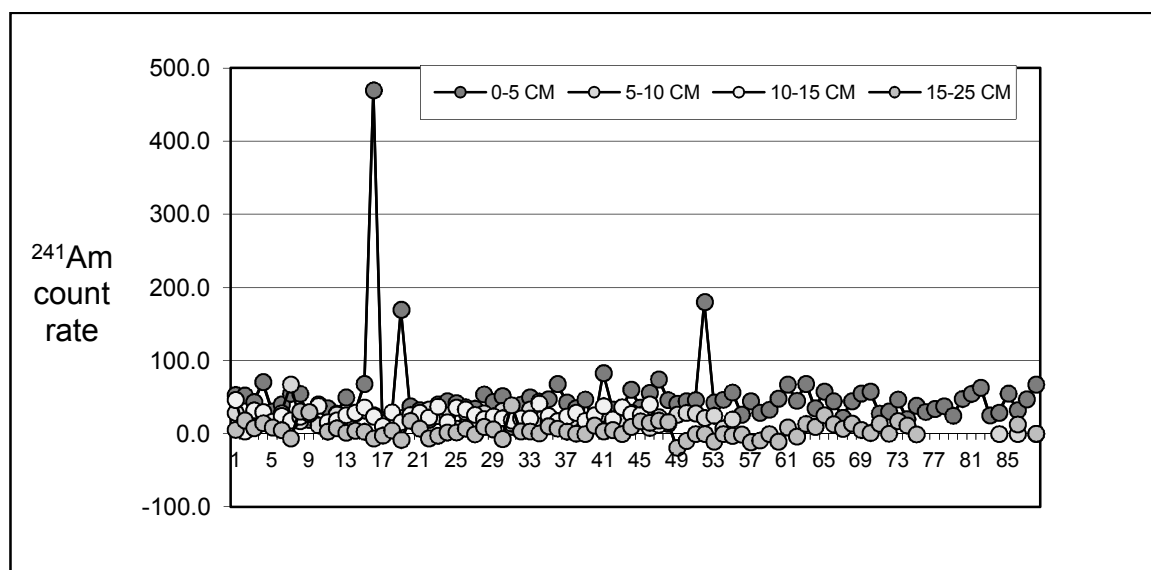
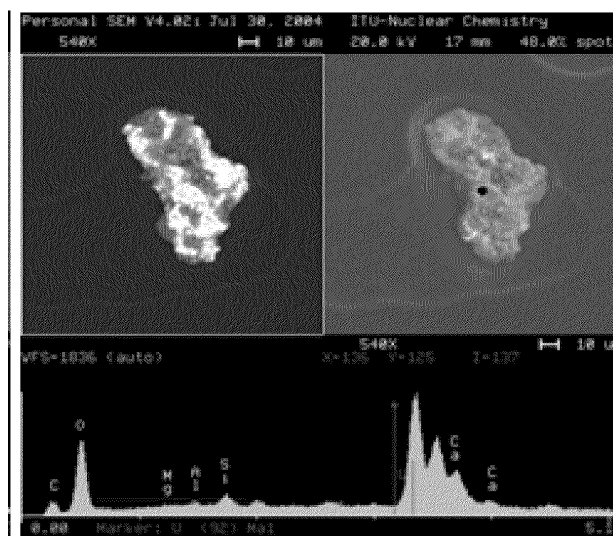
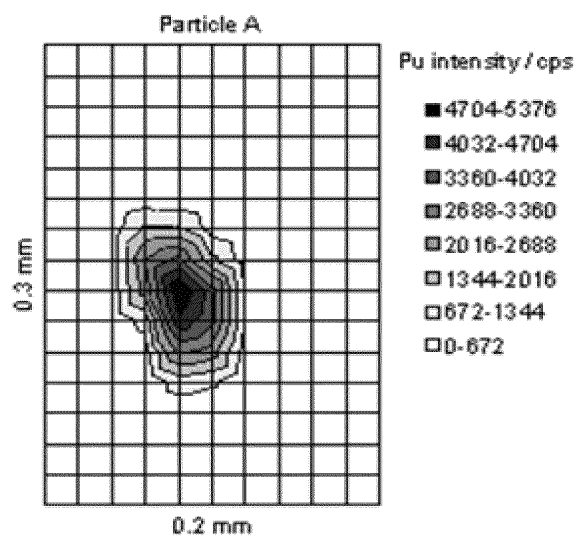


Figure 2



2a.



2b.

TABLE 1

Field Log #	Location Information	Activity Concentration (Bq kg <sup>-1</sup> , dry soil)				<sup>240</sup> Pu/ <sup>239</sup> Pu atom ratio
		<sup>137</sup> Cs	<sup>241</sup> Am	<sup>239</sup> Pu	<sup>239</sup> + <sup>240</sup> Pu	
00EY-01104	GRID PT. (0,0)	4.9 ± 0.4	225 ± 3	643 ± 5	795 ± 5	0.0642 ± 0.0003
00EY-01105	GRID PT. (2,0)	35.6 ± 0.5	204 ± 3	841 ± 12	1048 ± 13	0.0670 ± 0.0005
00EY-01106	GRID PT. (4,0)	33.8 ± 0.7	262 ± 5	1096 ± 8	1339 ± 8	0.0603 ± 0.0002
00EY-01107	GRID PT. (6,0)	43.5 ± 0.8	132 ± 5	1276 ± 9	1548 ± 9	0.0581 ± 0.0002
00EY-01108	GRID PT. (8,0)	47.8 ± 1.2	215 ± 3	1477 ± 4	1783 ± 5	0.0564 ± 0.0001
00EY-01109	GRID PT. (10,0)	20.7 ± 1.1	60 ± 2	391 ± 3	494 ± 3	0.0719 ± 0.0003
00EY-01110	GRID PT. (0,2)	20.1 ± 0.6	152 ± 5	542 ± 4	691 ± 4	0.0749 ± 0.0003
00EY-01111	GRID PT. (2,2)	52.4 ± 0.9	249 ± 3	1268 ± 18	1591 ± 19	0.0694 ± 0.0005
00EY-01112	GRID PT. (4,2)	52.6 ± 0.8	233 ± 2	831 ± 6	1060 ± 6	0.0750 ± 0.0003
00EY-01113	GRID PT. (6,2)	117 ± 1	193 ± 2	1125 ± 8	1504 ± 9	0.0917 ± 0.0003
00EY-01114	GRID PT. (8,2)	31.8 ± 0.7	183 ± 4	719 ± 2	890 ± 2	0.0645 ± 0.0002
00EY-01115	GRID PT. (10,2)	50.7 ± 0.5	219 ± 2	890 ± 13	1101 ± 13	0.0645 ± 0.0005
00EY-01116	GRID PT. (0,4)	115 ± 1	361 ± 2	1194 ± 9	1509 ± 9	0.0717 ± 0.0002
00EY-01117	GRID PT. (2,4)	33.2 ± 0.6	394 ± 3	1533 ± 11	1866 ± 11	0.0592 ± 0.0002
00EY-01118	GRID PT. (4,4)	32.2 ± 0.5	356 ± 2	1736 ± 13	2111 ± 13	0.0588 ± 0.0002
00EY-01119	GRID PT. (6,4)	28.2 ± 0.8	310 ± 5	1328 ± 19	1618 ± 20	0.0594 ± 0.0004
00EY-01120	GRID PT. (8,4)	26.7 ± 0.6	174 ± 4	1086 ± 8	1324 ± 8	0.0595 ± 0.0002
00EY-01121	GRID PT. (10,4)	25.9 ± 0.7	108 ± 2	978 ± 12	1191 ± 12	0.0591 ± 0.0005
00EY-01122	GRID PT. (0,6)	10.6 ± 0.4	160 ± 3	706 ± 7	856 ± 8	0.0578 ± 0.0005
00EY-01123	GRID PT. (2,6)	10.5 ± 0.5	247 ± 2	1013 ± 3	1226 ± 4	0.0571 ± 0.0003
00EY-01124	GRID PT. (4,6)	34.2 ± 0.7	529 ± 4	582 ± 4	711 ± 4	0.0605 ± 0.0002
00EY-01125	GRID PT. (6,6)	31.8 ± 0.6	387 ± 5	1926 ± 8	2331 ± 8	0.0573 ± 0.0001
00EY-01126	GRID PT. (8,6)	8.8 ± 0.4	316 ± 3	1432 ± 6	1738 ± 6	0.0580 ± 0.0001
00EY-01127	GRID PT. (10,6)	7.6 ± 0.4	414 ± 5	2301 ± 15	2781 ± 15	0.0567 ± 0.0002
00EY-01128	GRID PT. (0,8)	5.6 ± 0.4	291 ± 3	1452 ± 6	1752 ± 6	0.0561 ± 0.0001
00EY-01129	GRID PT. (2,8)	7.8 ± 0.3	522 ± 3	2532 ± 8	3059 ± 8	0.0567 ± 0.0001
00EY-01130	GRID PT. (4,8)	9.1 ± 0.4	442 ± 3	1675 ± 5	2030 ± 5	0.0577 ± 0.0001
00EY-01131	GRID PT. (6,8)	5.0 ± 0.3	353 ± 3	1642 ± 5	1994 ± 5	0.0583 ± 0.0001
00EY-01132	GRID PT. (8,8)	5.2 ± 0.9	142 ± 3	1038 ± 7	1271 ± 7	0.0609 ± 0.0003
00EY-01133	GRID PT. (10,8)	4.6 ± 0.6	202 ± 5	1030 ± 3	1263 ± 3	0.0614 ± 0.0001
00EY-01134	GRID PT. (0,10) <sup>#</sup>	7.2 ± 0.2	203 ± 2	765 ± 2	926 ± 3	0.0573 ± 0.0001
00EY-01135	GRID PT. (2,10) <sup>#</sup>	3.9 ± 0.5	203 ± 4	931 ± 6	1136 ± 6	0.0600 ± 0.0003
00EY-01136	GRID PT. (4,10) <sup>#</sup>	3.0 ± 0.3	194 ± 3	898 ± 5	1093 ± 6	0.0590 ± 0.0004
Arithmetic Mean & Standard Deviation		30 ± 28	268 ± 119	1178 ± 490	1443 ± 587	0.062 ± 0.008
#These grid sample sites located on ocean beach were excluded from summary statistics						

**TABLE 2.**

<b>Site/Depth</b>	<b><math>^{239+240}\text{Pu}</math> Bq kg<sup>-1</sup>, dry wt.</b>	<b><math>^{240}\text{Pu}/^{239}\text{Pu}</math> atom ratio</b>
<b>Site 1</b>		
0-5 cm	2.08 ± 0.022	0.0717 ± 0.0003
5-10 cm	1.74 ± 0.021	0.0696 ± 0.0003
10-15 cm	1.06 ± 0.006	0.0727 ± 0.0001
15-20 cm	2.02 ± 0.012	0.0671 ± 0.0001
<b>Site 2</b>		
0-5 cm	1.91 ± 0.005	0.0583 ± 0.0002
5-10 cm	0.99 ± 0.006	0.0645 ± 0.0006
10-15 cm	0.85 ± 0.004	0.0544 ± 0.0010
15-20 cm	0.13 ± 0.001	0.0577 ± 0.0016
<b>Site 3</b>		
0-5 cm	1.91 ± 0.007	0.0542 ± 0.0010
5-10 cm	0.87 ± 0.005	0.0619 ± 0.0001
10-15 cm	0.97 ± 0.011	0.0588 ± 0.0002
15-20 cm	0.01 ± 0.000	0.0668 ± 0.0014
<b>Site 4</b>		
0-5 cm	3.15 ± 0.021	0.0563 ± 0.0003
5-10 cm	5.18 ± 0.073	0.0547 ± 0.0006
10-15 cm	1.79 ± 0.011	0.0577 ± 0.0001
15-20 cm	1.44 ± 0.011	0.0604 ± 0.0001
<b>Site 5</b>		
0-5 cm	4.63 ± 0.028	0.0563 ± 0.0003
5-10 cm	4.46 ± 0.027	0.0551 ± 0.0001
10-15 cm	4.16 ± 0.029	0.0551 ± 0.0001
15-20 cm	4.97 ± 0.036	0.0563 ± 0.0001

**TABLE 3**

<b>Isotope</b>	<b>Isotopic Abundance (Atom %)</b>	<b>Alpha Activity (%)</b>
<sup>238</sup> Pu	0.011%	2.5%
<sup>239</sup> Pu	94.0%	79.1%
<sup>240</sup> Pu	6.0%	18.4%
<sup>241</sup> Pu	0.051%	0.0017%
<sup>242</sup> Pu	0.023%	0.0013%
<sup>244</sup> Pu	0.003%	$7 \times 10^{-9}$
<hr/>		
<sup>234</sup> U	0.006%	52.7%
<sup>235</sup> U	0.73%	2.1%
<sup>236</sup> U	0.0001%	0.005%
<sup>238</sup> U	99.26%	45.2%
reference date, 1 January 2005		

TABLE 4

Sieve Size	% soil	Activity Concentration, Bq kg <sup>-1</sup>		<sup>240</sup> Pu/ <sup>239</sup> Pu atom ratio	% <sup>239+240</sup> Pu
		<sup>239</sup> Pu	<sup>239+240</sup> Pu		
<b>00EY-01088, 0-5 cm</b>					
Bulk	100.00	1798 ± 28	2187 ± 28	0.0586 ± 0.0002	100%
< 20 µm	0.6 ± 0.2	3530 ± 34	4296 ± 35	0.0588 ± 0.0001	2.5%
20–44 µm	2.1 ± 0.2	3265 ± 63	3973 ± 65	0.0588 ± 0.0002	7.7%
44–125 µm	7.4 ± 0.7	2156 ± 22	2640 ± 23	0.0609 ± 0.0001	18.1%
125–500 µm	55.8 ± 4.3	987 ± 32	1195 ± 32	0.0572 ± 0.0003	61.7%
500 µm–1.2 mm	13.7 ± 0.5	496 ± 5	603 ± 5	0.0585 ± 0.0002	7.7%
1.2-4.8 mm	8.5 ± 0.5	137 ± 3	168 ± 3	0.0623 ± 0.0005	1.3%
>4.75 mm	11.8 ± 4.8	70 ± 1	89 ± 1	0.0756 ± 0.0006	1.0%
<b>00EY-01089, 5-10 cm</b>					
Bulk	100.00	1343 ± 21	1660 ± 21	0.0640 ± 0.0005	100%
< 20 µm	0.2 ± 0.1	1854 ± 27	2285 ± 28	0.0630 ± 0.0002	0.6%
20–44 µm	2.2 ± 0.5	1388 ± 22	1714 ± 23	0.0636 ± 0.0005	5.9%
44–125 µm	8.2 ± 0.9	1509 ± 23	1853 ± 24	0.0619 ± 0.0002	24.2%
125–500 µm	36.6 ± 1.6	745 ± 11	914 ± 11	0.0615 ± 0.0002	53.6%
500 µm–1.2 mm	16.7 ± 0.2	335 ± 6	414 ± 6	0.0640 ± 0.0003	11.0%
1.2-4.8 mm	15.0 ± 1.3	72 ± 1	92 ± 1	0.0743 ± 0.0008	2.2%
>4.75 mm	21.4 ± 1.2	54 ± 1	68 ± 1	0.0698 ± 0.0008	2.3%
<b>00EY-01100, 0-5 cm</b>					
Bulk	100.00	2583 ± 43	3109 ± 44	0.0553 ± 0.0002	100%
< 20 µm	0.3 ± 0.1	11436 ± 134	13766 ± 137	0.0553 ± 0.0001	1.2%
20–44 µm	1.0 ± 0.1	9725 ± 274	11699 ± 280	0.0551 ± 0.0004	3.0%
44–125 µm	4.6 ± 0.1	4460 ± 91	5380 ± 93	0.0560 ± 0.0001	6.5%
125–500 µm	75.8 ± 1.1	3366 ± 320	4058 ± 327	0.0557 ± 0.0009	81.1%
500 µm–1.2 mm	13.4 ± 0.2	1762 ± 112	2121 ± 115	0.0554 ± 0.0006	7.5%
1.2-4.8 mm	2.3 ± 0.3	723 ± 56	874 ± 57	0.0565 ± 0.0014	0.5%
>4.75 mm	2.6 ± 0.9	272 ± 12	328 ± 13	0.0562 ± 0.0009	0.2%
<b>00EY-01092, 0-5 cm</b>					
Bulk	100.00	3985 ± 60	4838 ± 62	0.0580 ± 0.0004	100%
< 20 µm	0.7 ± 0.6	4395 ± 45	5327 ± 46	0.0575 ± 0.0001	2.9%
20–44 µm	2.4 ± 0.0	3621 ± 36	4396 ± 37	0.0580 ± 0.0001	7.9%
44–125 µm	7.4 ± 0.8	2093 ± 28	2547 ± 29	0.0590 ± 0.0001	14.4%
125–500 µm	53.4 ± 2.5	1282 ± 20	1554 ± 20	0.0575 ± 0.0002	63.4%
500 µm–1.2 mm	18.3 ± 1.2	527 ± 8	642 ± 8	0.0597 ± 0.0002	9.0%
1.2-4.8 mm	10.7 ± 1.4	199 ± 3	244 ± 3	0.0605 ± 0.0003	2.0%
>4.75 mm	7.2 ± 1.4	58 ± 1	71 ± 1	0.0596 ± 0.0006	0.4%
<b>00EY-01096, 0-5 cm</b>					
Bulk	100.00	2669 ± 19	2669 ± 45	0.0563 ± 0.0003	100%
< 20 µm	0.4 ± 0.2	12718 ± 176	15395 ± 176	0.0573 ± 0.0003	0.4%
20–44 µm	1.3 ± 0.2	10789 ± 149	13053 ± 150	0.0572 ± 0.0002	1.3%
44–125 µm	5.8 ± 0.5	3440 ± 48	4171 ± 45	0.0587 ± 0.0002	6.0%
125–500 µm	74.3 ± 1.1	1757 ± 22	2115 ± 42	0.0573 ± 0.0002	74.5%
500 µm–1.2 mm	13.7 ± 1.1	1073 ± 14	1291 ± 23	0.0561 ± 0.0002	13.4%
1.2-4.8 mm	2.5 ± 0.1	236 ± 3	290 ± 38	0.0554 ± 0.0002	2.5%
>4.75 mm	2.1 ± 0.8	66 ± 1	82 ± 15	0.0564 ± 0.0003	2.0%



